Fitoterapia 82 (2011) 777–781

Contents lists available at ScienceDirect

Fitoterapia

journal homepage: www.elsevier.com/locate/fitote

Chemical constituents from endophytic fungus *Fusarium oxysporum*

Quan-Xin Wang [a,b], Sai-Fei Li [b], Feng Zhao [c], Huan-Qin Dai [b], Li Bao [b], Rong Ding [d], Hao Gao [d], Li-Xin Zhang [b,*], Hua-An Wen [b], Hong-Wei Liu [b,*]

[a] *School of Life Science, University of Science and Technology of China, No. 96 Jinzhai Road, Hefei, 230026, PR China*
[b] *Key Lab of Systematic Mycology and Lichenology, Institute of Microbiology, Chinese Academy of Sciences, No.8 Beiertiao, Zhongguancun, Haidian District, Beijing, 100090, PR China*
[c] *School of Pharmacy, Yantai University, No. 32 Qingquan Road, Laishan District, Yantai, 264005, PR China*
[d] *Institute of Traditional Chinese Medicine and Natural Products, College of Pharmacy, Jinan University, Guangzhou, 510632, PR China*

ARTICLE INFO

Article history:
Received 16 February 2011
Accepted in revised form 23 March 2011
Available online 9 April 2011

Keywords:
Fusarium oxysporum
Oxysporidinone analogues
Cytotoxicity
Antibacterial

ABSTRACT

A new oxysporidinone analogue (1) and a new 3-hydroxyl-2-piperidinone derivative (2), along with the known compounds (−)-4,6′-anhydrooxysporidinone (3), (+)-fusarinolic acid (4), gibepyrone D (5), beauvercin (6), cerevisterol (7), fusaruside (8), and (2*S*,2′*R*,3*R*,3′*E*,4*E*,8*E*)-1-*O*-D-glucopyranosyl-2-*N*-(2′-hydroxy-3′-octadecenoyl)-3-hydroxy-9-methyl-4,8-sphingadienine (9) were isolated from *Fusarium oxysporum*. Compounds 1–9 were evaluated for cytotoxicity using the MTT method against cancer cell lines, PC-3, PANC-1, and A549. Beauvericin showed cytotoxicity against PC-3, PANC-1, and A549 with IC_{50} value of 49.5 ± 3.8, 47.2 ± 2.9, and 10.4 ± 1.6 μM, respectively. Beauvericin also exhibited anti-bacterial activity towards methicillin-resistant *Staphylococcus aureus* (MIC = 3.125 μg/mL) and *Bacillus subtilis* (MIC = 3.125 μg/mL).

1. Introduction

Endophytic fungi can be found inhabiting the living internal tissues of some plants, often without causing any obvious negative effects or external symptoms. They have been found to be promising sources of new and biologically active natural products which are of interest for specific medicinal or agrochemical applications [1]. In the course of our ongoing efforts to discover potential anticancer agents from fungi, the EtOAc extract from an endophytic strain of *Fusarium oxyporum* showed cytotoxicity against cancer cell line A549. The endophytic fungus *F. oxyporum* was isolated from the bark of *Cinnamomum kanehirae*, an endemic plant of Taiwan. *C. kanehirae* (Bull camphor tree) is the only host plant for a well-known Chinese medicinal fungus of *Antrodia camphorates* that parasitizes on the inner cavity of the *C. kanehirae*.

Previous investigations have proved that fungi of the genus *Fusarium* are a rich source of biologically active secondary metabolites, including the anti-fungal agents oxysporidinone [2] and 6-*epi*-oxysporidinone [3], antimicrobial agents beauvericin and bikaverin [4], fungal toxins fumonisin [5] and sambutoxin [6], phosphatidylinositide 3-kinase inhibitor wortmannin [7], and immunosuppressive agent cyclosporine A [8]. In the study presented here, the chemical investigation of an EtOAc extract of a solid *F. oxysporum* culture led to the isolation of two new compounds, a new oxysporidinone analogue (1) and a new 3-hydroxyl-2-piperidinone derivative (2), along with the known compounds (−)-4,6′-anhydrooxysporidinone (3) [9], (+)-fusarinolic acid (4) [10], gibepyrone D (5) [11], beauvericin (6) [12], cerevisterol (7) [13], fusaruside (8) [13], (2*S*,2′*R*,3*R*,3′*E*,4*E*,8*E*)-1-*O*-D-glucopyranosyl-2-*N*-(2′-hydroxy-3′-octadecenoyl)-3-hydroxy-9-methyl-4,8-sphingadienine (9) [14] (Fig. 1). Details of the isolation, structural determination of two new compounds, and their cytotoxicity and antimicrobial activities are presented herein.

2. Experimental

2.1. Fungal material

The culture of *F. oxysporum* was isolated from the bark of *C. kanehirae* from Jiaoban Mountain, Taiwan Province, in

* Corresponding authors. Tel.: +86 10 62566577; fax: +86 10 62566511.
E-mail address: liuhw@im.ac.cn (H.-W. Liu).

0367-326X/$ – see front matter © 2011 Elsevier B.V. All rights reserved.
doi:10.1016/j.fitote.2011.04.002

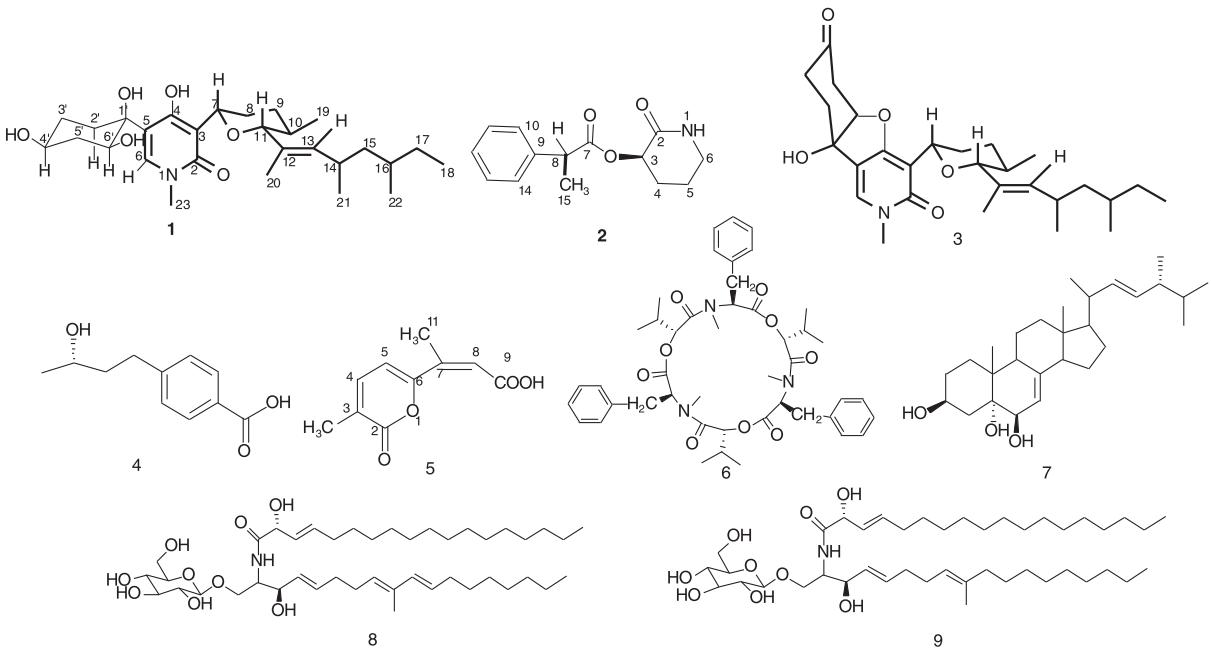

Fig. 1. Structures of compounds 1–9 from an endophytic strain of *Fusarium oxyporum*.

October 2009. The fungus was identified by observing the morphological characteristics and analysis of the internal transcribed spacer (ITS) regions (GenBank accession number GU250648), and assigned the accession number 633 in culture collection at the Institute of Microbiology, Chinese Academy of Sciences, Beijing. The fungal strain was cultured on slants of potato dextrose agar at 25 °C for 10 days. Agar plugs were inoculated in 500 mL Erlenmeyer flask containing 120 mL of media (0.4% glucose, 1% malt extract, and 0.4% yeast extract). The final pH of the media was adjusted to 6.5 before sterilization. The agar pugs in media were then incubated at 25 °C on a rotary shaker at 170 rpm for one week. Large scale fermentation was carried out in twenty 500 mL Fernbach flasks each containing 80 g of rice and 120 mL of distilled H_2O. Each flask was inoculated with 5.0 mL of the culture medium and incubated at 25 °C for 40 days.

2.2. General

Optical rotations were measured on a Perkin–Elmer 241 polarimeter. UV spectra were obtained with a Shimadzu UV2401PC UV–Vis recording spectrophotometer in MeOH. ESI-MS was conducted using a Bruker esquire 2000 mass spectrometer. HRTOFMS spectra were measured on a Bruker microTOF-Q instrument. ^1H and ^{13}C NMR, along with 2D NMR spectra, were obtained on a Bruker AV-500 NMR spectrometer (500 MHz for ^1H, 125 MHz for ^{13}C), using TMS as an internal standard. Chemical shifts were expressed in δ (ppm) and coupling constants (J) were reported in hertz (Hz). TLC was carried out on Silica gel $60F_{254}$ and the spots were visualized by spraying with 10% H_2SO_4 and heating. LH-20 (Amersham Biosciences) and ODS (40–63 μm, Merck) were used for column chromatography. Preparative HPLC was performed on a Agilent 1200 HPLC system using an ODS column (YMC-Pack C18, 250 × 10 mm, 5 μm) with a flow rate of 3.0 mL/min.

2.3. Extraction and isolation

The fermented rice substrate was extracted repeatedly with EtOAc (3 × 1 L), and the organic solvent was completely evaporated under vacuum to afford the crude extract. The crude extract was then suspended in water (1 L) and partitioned with n-hexane (3 × 1 L) and CH_2Cl_2 (3 × 1 L), successively. The CH_2Cl_2-soluble fraction (5.59 g) was subjected to Sephadex LH-20 chromatography using MeOH as the eluent to give 5 fractions (A–E). Fraction B was purified by RP-HPLC with 98% MeOH in water to afford compound 8 (5.7 mg, t_R 33.4 min) and compound 9 (10.8 mg, t_R 38.4 min). Fraction C was separated by silica gel column chromatography using $CHCl_3$–MeOH gradient elution (1% to 50%) to afford 16 subfractions (C1–C16). The subfraction C10 was separated on an ODS column using MeOH–H_2O gradient elution (30%, 50%, 70%, and 90% MeOH in water) to yield ten subfractions (C10-1 to C10-10). Compound 5 (10.4 mg) was purified from the fraction C10-2 by sephadex LH-20 using MeOH as the eluent. The subfraction C10-5 was isolated by RP-HPLC using 73% acetonitrile in water to give compound 6 (17.5 mg, t_R 34.8 min). The fraction C13 was subjected to ODS column chromatography using MeOH–H_2O gradient elution (30%, 50%, 70%, and 90% MeOH in water) to give nine subfractions (C13-1 to C13-9). Compound 4 (170 mg) was obtained from the subfraction C13-1 by sephadex LH-20 column chromatography with MeOH as the eluent. The subfractions C13-5 and C13-7 were subjected to RP-HPLC to give compound 3 (78% MeOH in water, 2.3 mg, t_R 23 min) and 7 (85% MeOH in water, 3.4 mg, t_R 48.4 min), respectively. Compounds 1 (80% MeOH in water, 7.5 mg, t_R 9.4 min) and 2 (28% acetonitrile in

water, 6.3 mg, t_R 13.8 min) were isolated by RP-HPLC from fractions C14 and C12, respectively.

2.3.1. Compound 1

Colorless crystalline; [α]25 D –42.5 (c 0.5, MeOH); UV (MeOH) λ_{max} nm (log ε): 215 (3.70), 290 (3.55); IR (neat) 3371, 2957, 2925, 2868, 1647 (C═O), 1551, 1454, 1388, 1296, 1228, 1150, 1030, 876, 734 cm^{-1};Positive ESI-MS: *m/z* 492 $[M+H]^+$, 514 $[M+Na]^+$; Negative ESI-MS:*m/z* 490 $[M-H]^-$; Positive HRTOFMS: *m/z* $[M+H]^+$ 492.3317 (calcd. for $C_{28}H_{46}NO_6$, 492.3320); for ^1H and ^{13}C NMR spectroscopic data see Table 1.

2.3.2. Compound 2

Amorphous solid; [α]25 D −100.5 (c 0.5, MeOH); UV (MeOH) λ_{max} nm (log ε): 208 (3.45), 220 (3.65); CD (MeOH) λ_{max} (Δε) 213 (−4.67), 224 (−32.5) nm; IR (neat) 3453, 2978, 2880, 1730 (C═O), 1622 (C═O), 1464, 1307, 1192, 1064, 915, 762, 702 cm^{-1}; Positive ESI-MS: *m/z* 248 $[M+H]^+$, 270 $[M+Na]^+$; Positive HRTOFMS: *m/z* $[M+H]^+$ 248.1275 (calcd. for $C_{14}H_{18}NO_3$, 248.1281); for ^1H and ^{13}C NMR spectroscopic data see Table 2.

2.3.3. Gibepyrone D (5)

Colorless crystalline; UV (MeOH) λ_{max} nm (log ε): 205 (3.45), 220 (3.65); IR(neat) 2955, 1726(C═O), 1600, 1432, 1371, 1294, 1238, 1122, 1062, 952, 882, 842, 761, 688 cm^{-1}; Positive ESI-MS: *m/z* 195 $[M+H]^+$, 217 $[M+Na]^+$; Negative ESI-MS:*m/z* 193 $[M-H]^-$, 387 [2 M–H]$^-$; HR-TOF-MS: *m/z* $[M+H]^+$ 195.0650 (calcd. for $C_{10}H_{11}O_4$, 195.0652); for ^1H and ^{13}C NMR spectroscopic data see Table 2.

Table 1
NMR data for compound 1 and (−)-oxysporidinone(500 MHz, in CD_3OD).

No.	δ_C	1	(−)-oxysporidinone [a]
		δ_H mult., *J* in Hz	δ_C
2	163.2		163.3,
3	111.2		111.2,
4	164.2		163.7
5	119.1		118.1
6	138.3	7.62 (*s*)	138.4
7	79.1	4.91 (*dd*, 10.0, 2.0 Hz)	79.1
8	30.6	1.58–1.62 (*m*), 1.94–1.97 (*m*)	31.52
9	33.2	1.44–1.47 (*m*), 1.94–1.97 (*m*)	33.2
10	33.7	1.75–1.77 (*m*)	33.7
11	93.6	3.54 (*d*, 10.0 Hz)	93.6
12	132.0		132.0
13	138.6	5.27 (*d*, 10.0 Hz)	138.7
14	30.9	2.54–2.61 (*m*)	30.9
15	46.1	1.12–1.15 (*m*), 1.24–1.27 (*m*)	46.1
16	33.0	1.34–1.37 (*m*)	33.4
17	29.8	1.07–1.10 (*m*), 1.44–1.47 (*m*)	29.8
18	11.6	0.88 (*d*, 6.5 Hz)	11.6
19	18.0	0.80 (*d*, 7.0 Hz)	18.0
20	12.6	1.70 (*d*, 2 .0 Hz)	12.5
21	21.2	0.96 (*d*, 7.0 Hz)	21.2
22	20.2	0.88 (*d*, 6.5 Hz)	20.2
23	37.7	3.51 (*s*)	37.8
1′	74.9		74.8
2′	40.1	1.76–1.79 (*m*), 2.38–2.40 (*m*)	32.8
3′	33.0	1.68–1.71 (*m*), 1.76–1.79 (*m*)	37.2
4′	69.4	3.65–3.68 (*m*)	212.1
5′	33.4	1.76–1.79 (*m*), 2.01–2.04 (*m*)	47.0
6′	70.5	4.32 (*dd*, 4.5, 11.5 Hz)	71.5

[a] Literature data reported in reference [9].

Table 2
NMR data for compound 2 (500 MHz, in $CDCl_3$) and 5(500 MHz, in CD_3OD).

No.	δ_C	2		δ_C	5
		δ_H mult., *J* in Hz			δ_H mult., *J* in Hz
2	173.2		2	165.1	
3	60.2	4.56 (*dd*, 3.3, 8.0 Hz)	3	128.8	
4	27.6	1.90–1.93 (*m*); 2.29–2.32 (*m*)	4	142.1	7.39 (*dd*, 7.2, 0.9 Hz)
5	24.7	1.82–1.85 (*m*); 1.98–2.02 (*m*)	5	108.0	6.68 (*d*, 7.2 Hz)
6	47.5	3.18–3.22 (*m*); 3.62–3.64 (*m*)	6	159.5	
7	175.5		7	144.3	
8	45.1	3.82 (*q*, 7.0 Hz)	8	121.1	6.61 (*s*)
9	140.3		9	170.4	
10/14	129.0	7.32–7.35 (*m*)	3-CH_3	17.5	2.10 (*d*, 0.9 Hz)
11/13	127.5	7.26–7.29 (*m*)	7-CH_3	14.5	2.36 (*d*, 1.0 Hz)
12	127.2	7.26–7.29 (*m*)			
15	20.1	1.48 (*d*, 7.0 Hz)			

2.4. Cytotoxicity bioassay

PC-3, PANC-1, and A549 cells were seeded in 96-well microtiter plates at 1200 cells/well. After 24 h, the compounds were added to the cells. After 48 h of drug treatment, cell viability was determined by measuring the metabolic conversion of MTT (3-[4,5-dimethylthiazol-2-yl]-2,5-diphenyltetrazolium bromide) into purple formazan crystals by active cells. MTT assay results were read using a microplate reader (Bio-Rad) at 570 nm. All compounds were tested at five concentrations and were dissolved in 100% DMSO to give a final DMSO concentration of 0.1% in each well. Each concentration of the compounds was tested in three parallel wells. IC_{50} values were calculated using Microsoft Excel software.

2.5. Antimicrobial assay

Fresh Mueller–Hinton broth medium (40 μL) and 2 μL of the test sample were added to each well of a sterilized 96-well microtiter plate followed by addition of 40 μL of the test strain culture including methicillin-resistant *Staphylococcus aureus* and *Bacillus subtilis* to each well. The plate was incubated at 37 °C overnight, and antimicrobial activity of samples was determined by measuring and comparing the optical density of the blank control and tested wells.

3. Results and discussion

The endophytic strain of *F. oxysporum* was fermented on rice medium. The EtOAc extract of the fermented rice substrate showed cytotoxicity against A549 cell line. Compounds 1–9 were isolated by a combination of column chromatography (silica gel, LH-20, and ODS) and HPLC purification as described in experimental section.

Compound 1 was assigned the molecular formula of $C_{28}H_{45}NO_6$ (seven degrees of unsaturation) on the basis of HRTOFMS and NMR data (Table 1). The ^1H and ^{13}C NMR spectra of 1 were very similar to those of (−)-oxysporidinone

except for the chemical shifts in the neighborhood of C-4′ and C-6′ [9]. An additional proton signal at δ 3.67 (m, H-4′) was observed in ^{1}H NMR spectrum of 1. A high-field signal at δ 69.4 (C-4′) appeared in its ^{13}C NMR spectrum instead of a carbonyl signal at δ 212.1 in (−)-oxysporidinone. This information, in combination with the molecular formula, revealed that compound 1 is a 4′-hydroxyl derivative of oxysporidinone at the C-4′ carbonyl moiety. The planar structure of 1 was further confirmed by ^{1}H–^{1}H COSY, HMQC, and HMBC spectral analysis (Fig. 2).

The relative stereochemistry of 1 was partially unraveled by determination of coupling constants and through-space proton–proton interactions (NOE) from the 2D-NOESY spectrum. Large coupling constants observed for H-6′ (11.5, 4.5 Hz) indicated that this proton is in an axial configuration. Strong NOE interactions between H-2′ and both H-6′ax and H-4′ identified protons in pseudo-axial positions (Fig. 2). The stereochemistry at C-1′ was evident from NOE interactions between H-6 (in the pyridone ring) and both H-6′ax and H-2′ ax, which can only be explained by placing the pyridone moiety above the plane of the cyclohexanone ring, that is, in the equatorial position.

Both H-7 and H-11 were determined to be axial on the basis of coupling constants (10.0 and 10.0 Hz, respectively). The large coupling constant of H-11 showed that H-10 is also in an axial configuration, indicating that CH_3-19 is in an equatorial position. The *E*-configuration for the double bond between C-12 and C-13 was established on the basis of the chemical shift of H-20 and further supported by the absence of a NOE correlation between H-20 and H-13. The difference in the chemical shifts of C-21 and C-22 (1.8 ppm) indicated that they are in an anti arrangement [15]. On the basis of above analysis, the full structure of compound 1 was established.

Compound 2 was obtained as an amorphous solid. The molecular formula was determined to be $C_{14}H_{17}NO_3$ by HR-TOF-MS and NMR (Table 2). The ^{1}H and ^{13}C NMR spectra of 2 indicated the presence of 2-phenylpropionate and 3-amino-2-piperidinone moieties. The 2-phenylpropionate group in 2 was revealed by proton signals due to a mono-substituted benzene ring [δ 7.55 (2 H, m, H-10, 14), 7.25 (3 H, m, H-11, 12, 13)], the methane signal at δ 3.82 (*q*, 7.0 Hz, H-8)), and the methyl signal at δ 1.48 (*d*, 7.0 Hz, H-15). Furthermore, ^{1}H–^{1}H COSY correlation between H-8 and H-15, and the HMBC correlations from H-15 to C-7, C-8, and C-9, and from H-8 to C-7, C-9, and C-10 confirmed the presence of a 2-phenylpropionate group. The presence of 3-amino-2-piperidinone was determined by ^{1}H–^{1}H COSY and HMBC spectra; the correlations between H-3 [δ 4.56 (*dd*, 3.3, 8.0 Hz)] and H-4 [δ 1.92 (m); 2.31 (m)], H-4 and H-5 [δ 1.83 (m); 2.00 (m)], H-5 and H-6 [δ 3.20 (m); 3.63 (m)], and the HMBC relationship between H-3 and C-2, C-4, and C-5 (Fig. 2). The HMBC correlations between H-3 and C-7 (δ 173.2) suggested that 2-phenylpropionate was connected to C-3 in 3-hydroxyl-2-piperidinone moiety through an ester bond.

The absolute configuration at C-3 in Fig. 2 was assigned by application of the CD method. The CD spectrum of 2 showed a negative Cotton effect at 224 nm arising from the 3-hydroxyl-2-piperidinone. The negative Cotton effect was consistent with that of 3(*R*)-amino-2-piperidinone [16], confirming the *R* configurations at C-3. The absolute configuration at C-8 was unresolved in this present study. Finally, the structure of 2 was determined to be 2-phenylpropionyl]-2-piperidinone-3 (*R*)-yl ester.

The full signal assignment for gibepyrone D (5) was achieved for the first time by 2D NMR spectral analysis (Table 2).

These oxysporidinone analogues constitute new members of a group of secondary metabolites from fungi with 4-hydroxy-2-pyridone chromophore. To date, five oxysporidinone analogues including oxysporidinone, 6-*epi*-oxysporidinone (the dimethyl ketal of oxysporidinone), (−)-4,6′-anhydrooxysporidinone, and (−)-6-deoxy oxysporidinone have been isolated from cultures of *Fusarium oxysporum*[2,3,9]. Oxysporidinone and 6-*epi*-oxysporidinone showed selective fungistatic activity against *Aspergillus fumigatus*[3].

3.1. Cytotoxicity

Compounds 1–9 were evaluated for *in vitro* cytotoxic activity against three human cancer cell lines, PC-3, PANC-1, and A549 by MTT method. Beauvericin was found to be the major cytotoxic agent contributing to the activity observed from the culture extract. Beauvericin showed cytotoxicity against PC-3, PANC-1, and A549 with IC_{50} value of 49.5 ± 3.8, 47.2 ± 2.9, and 10.4 ± 1.6 μM, respectively. The positive control, cisplatin, showed cytotoxicity against PC-3, PANC-1, and A549 with IC_{50} value of 26.8 ± 3.2, 26.2 ± 2.6, and 19.8 ± 2.4 μM, respectively. In comparison with the positive control, beauvericin presented strong selective cytotoxicity toward the A549 cell line. The other compounds isolated showed weak cytotoxic activity with IC_{50} value larger than 100 μM for all tested cell lines.

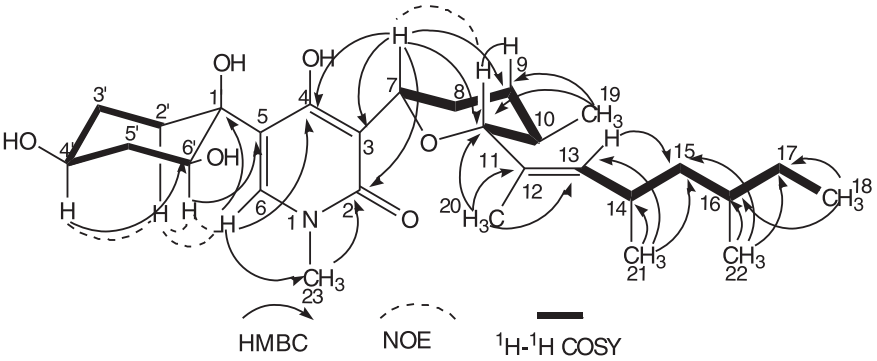

Fig. 2. Key HMBC, NOESY and ^{1}H–^{1}H COSY correlations for compound 1.

All isolates were also screened for their anti-bacterial activity against methicillin-resistant *S. aureus* (MRSA), clinical isolates from Beijing Chao-yang Hospital, and *B. subtilis* (BS) ATCC66333. Beauvericin showed strong anti-MRSA and anti-BS activity with the MIC value at 3.125 μg/mL, respectivley. (−)-4, 6′-anhydrooxysporidinone (3) showed weak anti-MRSA activity (MIC = 100 μg/mL) and moderate anti-BS activity (MIC = 25 μg/mL). All other compounds did not show any antimicrobial activity at the level of 100 μg/mL. It is the first report of anti-bacterial activity for oxysporidinone analogues.

Acknowledgements

This work was supported by the National Key Basic Research Project of China (2009CB522300) and MOST (2007DFB31620), and grants from Chinese Academy Science (KSCX2-YW-G-074-04).

References

[1] Schulz B, Boyle C, Draeger S, Rommert AK, Krohn K. Mycological Res 2002;106:996.
[2] Breinhold J, Ludvigsen S, Rassing BR. J Nat Prod 1997;60:33.
[3] Jayasinghe L, Abbas HK, Jacob MR. J Nat Prod 2006;69:439.
[4] Schneider P, Misiek M, Hoffmeister D. Mol Pharm 2008;5:234.
[5] Gelderblom WC, Jaskiewicz K, Marasas WF, Thiel PG, Horak RM, Vleggaar R, et al. Appl Environ Microbiol 1988;54:1806.
[6] Kim JC, Lee YW. Appl Environ Microbiol 1994;60:4380.
[7] Woscholski R, Kodaki T, McKinnon M, Waterfield MD, Parker PJ. FEBS Lett 1994;42:109.
[8] Rodríguez MA, Cabrera G, Godeas A. J Appl Microbiol 2006;100:575.
[9] Zhan J, Burns AM, Liu MX, Faeth SH, Gunatilaka AA. J Nat Prod 2007;70:227.
[10] Song JJ, Yee NK. J Org Chem 2001;66:605.
[11] Barrero AF, Oltra JE, Herrador MM. Tetrahedron 1993;49:141.
[12] Gupta S, Montllor C, Hwang YS. J Nat Prod 1995;58:733.
[13] Ceccherelli P, Fringuelli R, Madruzza GF, Ribaldi M. Phytochemistry 1975;14:1434.
[14] Shu RG, Wang FW, Yang YM, Liu YX, Tan RX. Lipid 2004;39:667.
[15] Organ MG, Bilokin YV, Bratovanov S. J Org Chem 2002;67:5176.
[16] Jiao Y, Yoshihara T, Ishikuri S, Uchino H, Ichihara A. Tetra Lett 1996;37:1039.